Atacama
Large
Millimeter
Array

Summary of the Second ALMA Phasing Project (APP) Commissioning and Science Verification Mission: 2015 March 24-30

ALMA Technical Note: Number 17
Status: Final

Prepared by:	Organization	Date
L. D. Matthews G. B. Crew	Massachusetts Institute of Technology Haystack Observatory	2015 September 4

MEMORANDUM

To: The ALMA Community

From: Lynn D. Matthews and Geoffrey B. Crew, MIT Haystack Observatory

Date: September 4, 2015

Subject: Summary of the second ALMA Phasing Project (APP) Commissioning and Science Verification mission: 2015 March 24-30

1 Background

The second Commissioning and Science Verification (CSV) mission for the ALMA Phasing Project (APP) was carried out during the ALMA Extension and Optimization of Capabilities (EOC) Week from 2015 March 24-30. The first APP CSV mission took place in 2015 January (hereafter referred to as the "January mission") and is summarized in ALMA Technical Note 16.[1] A highlight of the January mission was the first successful detection of a Very Long Baseline Interferometry (VLBI) fringe between ALMA and a fully independent station (the Atacama Pathfinder Experiment (APEX) telescope), demonstrating that all major hardware components of the ALMA Phasing System (APS) are fully operational. However, the signal-to-noise ratio of the detected fringe implied that ALMA was effectively operating as a single 12-m antenna rather than a phased array, a problem that was ultimately traced to a difference in the way various delays are applied to the data stream used to form the phased sum signal compared with the normal ALMA antennas (see ALMA Technical Note 16 for additional discussion).

Following the January mission, the APP Team developed a workaround for the delay problem. As a first step, an option was implemented to *turn off* the baseband delay applications in the correlator data processor (CDP) when executing an observing block (i.e., "useRDC=False"). This patch was tested during software regression testing in late January and verified to work as expected. As a second step, the APP's TelCal code was modified to create an arbitrary (power of two) number of channel averages in any given spectral window.[2],[3] The appropriate phase corrections for each individual antenna are computed independently for each of these channel averages, effectively allowing the APS software to solve for phase as a function of frequency. This in turn removes the phase ramp across each baseband caused by turning off the default delay corrections.

[1] https://almascience.nrao.edu/documents-and-tools/alma-technical-notes/

[2] While the APP software now allows an arbitrary number of channel averages per baseband, the maximum number permitted by ALMA Observing Tool (OT) is currently set to 10. An increase in this number to a value of 32 is slated to be implemented in late 2015.

[3] An alternative would be to use a larger number of spectral windows; however, the correlator does not currently perform well when using large numbers of spectral windows.

1.1 Objectives

The primary objective for the second APP CSV campaign was to test and characterize the phasing system, including the recent changes in the handling of the front-end delays. Secondary goals were to repeat the local VLBI test between ALMA and an antenna at the Operations Support Facility (OSF) (also attempted during the January mission) and to obtain a short VLBI recording on a calibrator source with ALMA and one or more stations operating as part of the Event Horizon Telescope (EHT) network, thus allowing demonstration of an intercontinental VLBI fringe.

1.2 Personnel

APP personnel on site during the 2015 March APP CSV mission included: Geoffrey Crew and Lynn Matthews (MIT Haystack Observatory); Matias Mora (NRAO); Alejandro Saez (JAO); and Helge Rottmann (MPIfR). The ALMA Science lead on site during the week was Anthony Remijan.

1.3 Impacts of Severe Weather

Northern Chile received record-setting rainfall during the early part of the 2015 March 24-30 EOC week. Blizzard conditions were present at the Array Operations Site (AOS), leading to a shutdown of operations. All internet and phone service were also disabled in Northern Chile for approximately one day. Clearing of the roadway leading to the AOS began on March 26, but owing to the roughly one meter of accumulated snow, ALMA personnel were not able to access the plateau and begin performing health checks on the antennas until March 28. Consequently, observations were possible only during the last two days of the EOC week.

2 Resources and Set-Ups Employed

2.1 Software Release

ALMA EOC activities during the week employed software version R2014.6. While the APP was nominally working on developments under R2015.2, to negate the need for software changes when switching between EOC and APP CSV activities, the APP opted to employ instead a backported branch of R2014.6 (APP-BACKPORT-2014-06-B). This branch contained all of the features needed by the APP. This branch was tested prior to the mission during the ALMA Department of Computing (ADC) regression test on March 23.

2.2 Antennas

ALMA was in a compact configuration during the mission, with maximum baselines of a few hundred meters. (The configuration was the same as during the January Mission). Because of snowfall (see §1.3), all antennas were stowed during the first five days of the EOC week and were unavailable for observing, except in simulation mode. On Day 6, 13

antennas became available, and 25 antennas became available on Day 7, but one of these lacked a Band 3 receiver and was excluded from the array used by the APP.

In addition, to the AOS antennas, antenna PM01 was parked on pad TF01 at the OSF and was nominally available for use by the APP for VLBI testing. However, ultimately it was not used during the March mission because of time constraints following the weather-related shutdown.

2.3 Remote VLBI Stations

During late March and early April 2015 (including dates overlapping with the March mission), the Event Horizon Telescope (EHT) project was engaged in a global VLBI campaign that included observations at 1.3 mm and 0.87 mm. Participating stations included the Combined Array for Research in Millimeter-wave Astronomy (CARMA), the James Clerk Maxwell Telescope (JCMT), the Submillimeter Array (SMA), the Submillimeter Telescope (SMT), the Large Millimeter Telescope (LMT), and the Institut de Radioastronomie Millimétrique (IRAM) 30-m telescope. ALMA was not formally part of this experiment. However, since obtaining intercontinental fringes in Band 6 between ALMA and other VLBI stations is part of the formal APP CSV plan, the staffing of these remote sites in parallel with the APP CSV campaign provided an ideal testing opportunity for the APP (see below).

2.4 Time Allocation

During the first five days of the EOC week, the APP observed in simulation mode only, collecting approximately two hours of simulation mode data on each day. (In this mode, the antennas do not point, but the receivers are powered on, and receiver noise is recorded). Approximately 10 hours of on-sky array time were allocated to the APP on Day 6 and 2 hours on Day 7, for a total of 12 hours on sky during the mission.

2.5 Data Collected

Observing targets for the mission comprised bright quasars selected from the ALMA Source Catalogue. Approximately 20 GB of ALMA standard interferometry mode (ASDM) data were collected in a combination of Bands 3, 6, and 7, and $\sim$1 TB of useful VLBI-mode data were recorded simultaneously with the ALMA interferometry mode data at selected times.

3 Results

3.1 Simulated Observations and Recorder Testing

Preliminary tests of the APP software used during the mission were performed using the SCO2 simulator in Santiago just prior to the start of the mission. Because of inclement

weather, the first five days of CSV activities were also limited to simulation mode observations, albeit with the real array. In contrast to the data produced by SCO2, which comprise only zeros, the simulated array data contain recorded receiver noise. These simulation mode tests allowed verification that the latest APP software could run without problems under normal observing conditions and that the system could be commanded in the manner required for phased ALMA observations. Various APP observing modes were tested (including those that exercised the fast and slow phasing loops independently and together). Other parameters were also varied, including the number of antennas in the array, the scan durations, the spectral set-ups, the numbers of spectral windows, and the number computed spectral averages. The readability and formatting integrity of the resulting uid data were then verified in CASA.

Among the things verified in simulation is that it is possible to carry out observations with up to 32 spectral averages per baseband and produce ASDM format data that can be read into CASA and processed in a normal manner, without any data formatting or CASA modifications. To test this, the baseline correlator Validator was patched to accept up to 32 channel average regions per spectral window. Following this, we were able to successfully execute manual mode simulated observations with 16 and 32 spectral averages per baseband, respectively. TelCal worked as expected with the output data, and we were also able to import the resulting ASDM files into CASA and perform standard operations on these data, demonstrating that no change to the ASDM model will be required to accommodate this change. We note that the ALMA Observing Tool (OT) currently limits the number of channel averages to 10, and the consequences of the increased data rate inherent in using larger numbers of channel averages has not yet been tested under real observing conditions, although no problems are anticipated once this capability becomes available in software release 2015.6 (see http://ictjira.alma.cl/browse/ICT-4656).

In addition to the software testing, the APP Mark 6 recorders were exercised during the shutdown time. During these recorder tests, we established that as a result of human error, the optical fiber link (OFL) had been disconnected. This was difficult to diagnose, as the network monitoring port on the device had been previously damaged, either due to accident or human error. Finally, a failing disk in one of the recorder modules required replacement. After correcting these issues, a 9.5-hour recording session showed nominal loss rates ($\sim$1 ppm).

3.2 On-Sky Observations: Checkout of the Phasing System – Session 1

The first on-sky tests became possible on March 29/30 (Day 6 of the mission), between 19:00-02:00 local time (22:00-05:00 UT; hereafter Session 1). An array of 12 12-m antennas was available; consequently, either 9 or 11 antennas were used in the phased array, along with either 1 or 3 unphased comparison antennas, respectively. The weather was stable and dry; the precipitable water vapor (PWV) at the start of the session was $\sim$1.1 mm and dropped to 0.56 mm near the end.

The highest priority goal of Session 1 was validation of the phasing software following several changes related to the handling of delays and the maximum number of spectral

averages for which phasing correlations can be computed per baseband (see §1 and §**??**).

3.2.1 USB/LSB Handling Issue

Examination of the first on-sky data obtained with the phasing system operating during Session 1 revealed that while the basebands associated with the lower sidebands (USB) were behaving as expected, the upper sidebands (USB) were applying phases incorrectly when using multiple TelCal phases (as is required when computing phase corrections for more than one channel average across a given baseband). It was quickly determined that this problem originated because of an ordering inconsistency between TelCal phases, tunable filterbank (TFB) filter frequencies, and channel average region center frequencies; VLBIObsControlHelper was reverting channel average frequencies according to USB/LSB, while AppUtilities::unpack was expecting them to be in the same (ascending) order as the two other parameters. A fix was implemented, installed, and tested during the session and was committed to software release 2014-06-B. The fix consisted of keeping all three parameters in ascending order before passing them to AppUtilities::unpack. After the full phase sequence is received back, the sign is reverted for USB before applying the correction.

3.2.2 Delay Corrections

Session 1 marked the first on-sky tests of the APP's workaround to the delay issue described above (§1) and in ALMA Technical Note 16. To exercise this option, the default delay corrections were turned off, and a modified version of the APP's TelCal code was deployed that allows solving for the phases in arbitrary numbers of channel averages within each correlator quadrant. During Session 1, tests with up to 8 channel averages per baseband were undertaken.

As seen in Figures 1 & 2, with this new method of handling the front-end delays implemented, acceptable phasing performance is now found in all four correlator quadrants, both polarizations, and in both Band 3 and Band 6. The left panels of Figures 1 & 2 show that for all polarization/baseband combinations, phases on baselines between antennas in the phased sum show a clear convergence toward zero (as expected for an unresolved point source) and a significant drop in RMS dispersion when the phasing solutions converge. At the same time that the phases converge toward zero, a marked increase in the correlated amplitude is observed in all quadrants and both polarizations on baselines between the phased sum and the (unphased) comparison antennas (right panels). Prior to the March campaign, a similar convergence of the phases toward zero was routinely seen in all quadrants/polarizations on baselines between antennas used to form the phased sum (e.g., Figure 3 of EOC Technical Memo 16); however, the corresponding jump in correlated amplitude was not present. The reason is that originally, the front-end delays were being applied in a correct manner to the "normal" ALMA antennas (i.e., to those shown in the left panels of Figures 1 & 2), but not to the phased sum signal or "sum antenna" itself, which is used to form the cross-correlation signals depicted in the right-hand panels of Figures 1 & 2.

In the case of the Band 6 data (Figure 2) we see that scatter in the phases is lowest immediately after phase-up, but then the data temporarily undergo some decorrelation,

leading to a systematic decrease in correlated amplitude, followed by a "recovery". It is unclear whether this behavior was due to a fluctuation in atmospheric conditions or some other cause.

3.2.3 Fast+Slow Loop Corrections

In addition to testing of the standard "slow" phasing loop (as for Figure 1 and 2), tests were also performed during Session 1 using the slow loop in conjunction with the "fast" phasing loop. The latter applies phase corrections on a shorter (∼1-second) cadence based on the path delays computed from the water vapor radiometer measurements obtained at each station. As seen in Figure 3, during the weather conditions of the March 30 observations, the RMS dispersion in the phases in Band 6 in each quadrant/polarization is lower ($\lesssim \pm 5^\circ$) compared with the slow loop alone (Figure 2), suggesting that the phasing algorithms themselves are performing with an efficiency approaching ∼99%.[4].

We note that Figure 3 exhibits two time intervals where the phases are identically zero. Such behavior was seen intermittently during the March campaign. Its origin is unclear, but it appears to be an ALMA software or firmware issue that is unrelated to the APS. The amplitudes and phases of the spectral data are also corrupted during affected scan. This problem is different from one that was documented previously in ICT JIRA ticket (ICT-3886), where only the channel-averaged data were zeroed, while the spectral data appeared to be normal.

3.2.4 Use of Multiple Channel Averages Per Baseband

One drawback of the method that the APP team has implemented to handle front-end delay corrections is that while the gross delays are well removed by solving in real time for phase as a function of frequency, these corrections are computed for only a finite number of frequency points across each baseband (i.e., one correction for each of the N_0 channel averages, where $N_0 \leq 8$ during our March tests). A consequence is that in some cases, the corrected cross-correlation spectra exhibit small residual phase ramps across each of the N_0 band segments, resulting in a "sawtooth" pattern (Figure 4). In practice, these phase slopes were found to range from roughly zero (i.e., imperceptible) to ∼0.1 turns across each of the individual segments. Because these phase ramps are relatively small, the resulting decorrelation losses are less than a few per cent. Consequently, we do not anticipate that this decorrelation will inhibit our ability to meet our formal phasing efficiency requirements. Nevertheless, we plan to explore further mitigating this effect by increasing the number of channel averages per baseband from ≤8 to 16 or 32. As noted above, we have successfully tested this in simulation, and this capability is expected to become available for routine on-sky testing in late 2015 (see ICT JIRA ticket ICT-4656).

[4]Because of quantization errors and other losses, this number does not reflect the *total* phasing efficiency of the systems; see §3.4.1

3.3 On-Sky Observations: Session 1 VLBI Fringe Tests

Within the first two hours of Session 1 it was established that the phasing system was performing well following the latest APP software updates. Given this satisfactory performance, coupled with favorable weather conditions, a decision was made to shift the focus of the session to attempting some VLBI recordings in parallel with the ongoing worldwide EHT observing campaign described above (§2.3). ALMA therefore joined various EHT sites in recording observations of the quasar 3C273, thereby providing an opportunity for VLBI fringe tests on >5000 km baselines with ALMA.[5] Indeed, such tests are specified as part of the formal APP CSV plan and are a natural follow-on to the successful fringe tests performed in 2015 January on the ∼2 km baseline between ALMA and APEX (see ALMA Technical Note 16).

APP observations that included VLBI recording were first attempted utilizing only two of the four correlator quadrants, each tuned to a center frequency commensurate with those adopted at other EHT sites. The other VLBI peer sites utilize a range of VLBI backends, but none presently matches the data rate of ALMA, hence this choice was made to minimize ALMA VLBI data volumes while producing data that could be correlated with peer sites in a straightforward manner. Unfortunately, two initial attempts to execute such VLBI scans failed for unknown reasons. During a subsequent attempt, real-time displays on the CorrGUI showed that the latest data exhibited artifacts in the form of a "porcupine" pattern in the cross-correlation amplitudes during certain scans, coupled with spurious phase values. As seen in Figure 5, these spurious amplitude and phase behaviors repeat within each of the 32 TFB channels. The origin and trigger of this behavior remains unknown. It is documented in an ICT JIRA ticket (ICT-4815) and has since been shown to be linked with use of the frequency division (FDM) observing modes, and to be independent of APP hardware and software.

Following these failures, observations were attempted again, this time commanding all four correlator quadrants, each tuned to the same center frequency of 227.10 GHz. This mode of operation at last produced data free of the corruption seen in the 2-quadrant mode data.[6] In the end, several successful VLBI scans were obtained on 3C273, and two short segments of data overlapped with successful VLBI recording on this source at other sites (04:05:00-04:07:16 UT and 04:40:00-04:43:12 UT). The stations with overlapping data included the IRAM 30-m antenna (Pico Veleta, Spain), the SMT (Mt. Graham, Arizona), and CARMA (Owens Valley, California).

3.4 On-Sky Observations: Session 2 Step Scans

A second APP observing session was carried out from 23:00-01:00 UT on March 30/31. Weather conditions were slightly less dry and stable than the previous night, with PWV ∼ 1.4 mm. During Session 2 there were 23 12-m antennas available, up to 19 of which were

[5]The data on baselines involving ALMA were obtained solely for APP CSV purposes and will not be distributed outside the APP team nor used in any manner by the EHT consortium.

[6]In fact, the number of correlator quadrants in use may have been immaterial; following the March mission, "porcupine" artifacts have also been seen in FDM data where all four quadrants were commanded (see ICT-4815).

used as part of the phased array. The objectives of this session were threefold: (1) validation of the performance of the phasing system with a sufficiently large number of antennas ($\geq$15) to permit testing of compliance with our formal requirements;[7] (2) additional testing of the fast loop phase corrections; (3) performance of "step scan" tests, as described in our formal CSV plan. For the latter tests, antennas are systematically added to or subtracted from the phased array, permitting evaluation of how the correlated amplitude and the phasing efficiency scale with the number of phased antennas in the array. In theory, the correlated amplitude should increase as $\sqrt{N_{\rm A}}$, where $N_{\rm A}$ is the number of phased antennas; however, the absolute value of the amplitude will also be affected by the overall phasing efficiency.

During Session 2, two "step scans", each of approximately 12 minutes duration, were executed in Band 6. These step scans began with an array of 19 phased antennas in all four correlator quadrants. Subsequently, pairs of antennas were sequentially removed from the phased array at arbitrary times during the execution block. The four correlator quadrants were modified independently, resulting in different numbers of phased antennas, $N_{\rm A}$, as a function of time for each quadrant. This type of exercise allows us to test how the performance and overall phasing efficiency of the system changes with different numbers of phased antennas.

Figure 7 shows sample step scan results for one baseband and polarization. The crosses indicate the correlated amplitude as a function of the number of phased antennas for a baseline between comparison antenna DA45 and the phased sum "antenna" during each 16-second scan. We see that the correlated amplitude scales as expected with the square root of the number of antennas in the phased sum for $N_{\rm A} < 19$, while for $N_{\rm A} = 19$, the measured amplitude appears to level off. However, given the limited number of antennas and measurements, additional observations will be need to confirm and fully evaluate this behavior. Further, while the relative amplitudes show approximately the expected "square root of $N_{\rm A}$" behavior as a function of the number of antennas in the phased array, a much more detailed and sophisticated analysis is required to gauge the actual *phasing efficiency*.

Losses in efficiency occur at two different stages in the APS. First, imperfect phasing solutions (e.g., due to atmospheric fluctuations, residual delay errors, and latency in the application of the phasing corrections) lead to a residual scatter, σ_ϕ, in the phases of all the corrected antennas used for form the phased sum. The decorrelation resulting from this residual scatter will produce a reduction in the correlated amplitude of the phased sum by a factor $\epsilon_0 \approx e^{\frac{-\sigma_\phi}{2}}$. For the data set shown in Figure 7, $\epsilon_0 \sim$0.93.

Ignoring gain differences between antennas, if we compute a vector average over all baselines between the phased antennas, the correlated amplitude that we derive, $\bar{A}'$, will therefore be ϵ_0 times the correlated amplitude expected for an ideal array of 2 phased antennas. The value of $\bar{A}'$ for baseband 1, polarization XX is shown as an asterisk on Figure 7. Assuming that correlated amplitude scales as the square root of the number of phased antennas, we may therefore extrapolate from this point the correlated amplitude expected for larger phased arrays—assuming that no further losses occur in the phasing system. This predicted relation in shown on Figure 7 as a dotted curve.

To compare with the dotted curve, the solid curve shown on Figure 7 shows a fit to

[7]One of the formal APP requirements is to demonstrate phase-up of with $\geq$90% efficiency for $\geq$15 antennas with baselines $\leq$2 km.

the actual measured values of the correlated amplitude on the baseline between the phased sum antenna and a comparison antenna for $11 \leq N_A \leq 19$. We see that the solid curve lies a factor of 0.89 below the dotted curve, implying that additional losses in efficiency have indeed occurred in forming the phased sum signal. To within uncertainties, this numerical factor matches the theoretical efficiency loss of 0.88 expected from the 2-bit quantization of the signal. We emphasize that the measurement represented by the asterisk on Figure 7 is unaffected by this loss, since it was derived using the signals from individual ALMA antennas, which unlike the sum signal, do not incur these extra quantization losses. In conclusion, *for the particular baseband and polarization shown in Figure 7, total losses in phasing efficiency are a combination of a ∼7% loss from imperfections in the phasing solutions and a numerical loss of ∼11% in forming the phased sum signal.* We note that there are some small uncertainties in these estimates resulting from the fact that gain optimization was not applied during most of the observations executed during the March campaign. Furthermore, we are still working on carefully confirming that normalization of the sum antenna is being handled correctly.

For some of the other baseband/polarization combinations in the data set shown in Figure 7, estimation of the phasing efficiency is complicated by at least one additional factor, namely that the comparison antenna—used to form cross-correlation prodcuts from which the correlated amplitude of the sum antenna is evaluated—receives no front-end delay corrections under our current implementation of the phasing system. Consequently, in the event that there happens to be a significant residual delay error for a particular baseband/polarization combination, the correlated amplitude will appear artificially low and the inferred phasing efficiency will appear lower than its true value. For the baseband/polarization combination shown in Figure 7, the phase gradient across the 1.875 GHz band is $\sim 5^\circ$, leading to negligible decorrelation. However, this is not the case for all of the baseband/polarization pairs, two of which show roughly half a turn of phase across the band. After correcting for these delay errors, we find similar efficiencies in all 8 baseband/polarization combinations.

4 Correlation of VLBI Data

Immediately following the mission, preliminary attempts to find VLBI fringes between ALMA and one of the other EHT sites using the DiFX software correlator proved unsuccessful. However, in mid-August, an issue was uncovered in the way that DiFX was handling the specified Earth Orientation Parameter. Following resolution of this issue, a fringe was detected in a segment of data on a baseline between ALMA and Pico Veleta (Figure 6). *This detection marks the first successful intercontinental VLBI fringe between ALMA and another station in any band.* Furthermore, it is the first successful VLBI fringe between a *phased* ALMA and an independent station. (During the VLBI fringe test with APEX in 2015 January, ALMA was effectively operating as a single antenna; see EOC Technical Memo 16).

5 Future and Ongoing Work

Subsequent to the fringe detection between ALMA and Pico Veleta with dual polarizations recorded at both stations, the correlated VLBI data were transferred to I. Martí-Vidal (Onsala) to allow testing of PolConvert, a tool that the APP team has been developing to handle the "mixed" polarizations obtained on VLBI baselines between ALMA (which records dual linear polarizations) and other VLBI sites (most of which record single or dual circular polarizations). PolConvert will operate by correcting the ALMA data at the post-correlation stage by computing and applying necessary corrections to the VLBI fringes and outputting circularly polarized data products in FITS-IDI format.

In parallel, analysis of the remaining VLBI scans obtained in 2015 March remains ongoing. Fringes were also detected with a second segment of data on the baseline between ALMA and Pico Veleta, but the signal-to-noise ratio is somewhat lower than in the scan shown in Figure 6. Most likely this is due to the low elevation of the source as observed from Pico Veleta ($\sim 20^\circ$ elevation compared with $\sim 27^\circ$ in the earlier data segment), but other possible causes should be ruled out. So far no fringes have been detected between ALMA and SMT, and the reason for this is also under investigation. Finally, only preliminary attempts have been made so far to search for fringes on the ALMA-CARMA baseline.

6 Summary

Despite extreme weather conditions that lead to a 5-day shutdown of ALMA operations, the APP was able to make important progress toward its CSV goals during the 2015 March 24 EOC week. Prior to this campaign, an issue with the manner in which front-end delays were applied to the data used to form the phased sum lead to significant decorrelation in all baseband/polarization/observing frequency combinations outside of quadrant 1, polarization XX in Band 3. A software workaround to this delay problem was successfully implemented, and the phasing system now appears to be working satisfactorily in both the XX and YY polarizations in all four correlator quadrants in Bands 3 and 6. Successful tests of the phasing system were executed with up to 19 phased antennas using both the slow and the fast phasing loops, as well as a combination of the two. Another major milestone was the first successful detection of a VLBI fringe with phased ALMA on an intercontinental baseline. Additional information on the 2015 March APP CSV mission is available on the mission wiki page:

https://ictwiki.alma.cl/twiki/bin/view/AppMissionChileCommissioning02 .

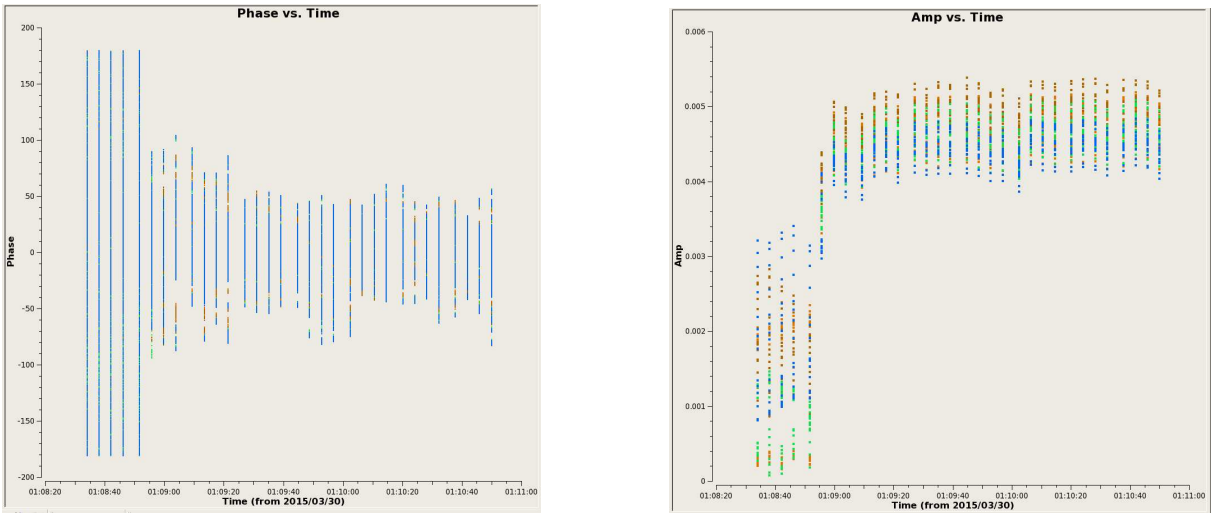

Figure 1: *Left:* phase as a function of time during Band 3 observations of the quasar 0522-364 on 2015 March 30. Only the slow phasing loop was active during this observation. All baselines between the 11 antennas in the phased sum are shown. Different colors indicate data from the four independent correlator quadrants. Data from both the XX and YY polarizations are shown within each quadrant. *Right:* correlated amplitude as a function of time for the same observation, for the baseline between the phased sum and an unphased comparison antenna. As seen in the left panel, phase-up occurs roughly 01:08:52 UT, or approximately 20 seconds after the start of the observation. At the corresponding time in the right-hand panel, the correlated amplitude significantly increases. Data source: uid://A002/X9cdda2/X245.

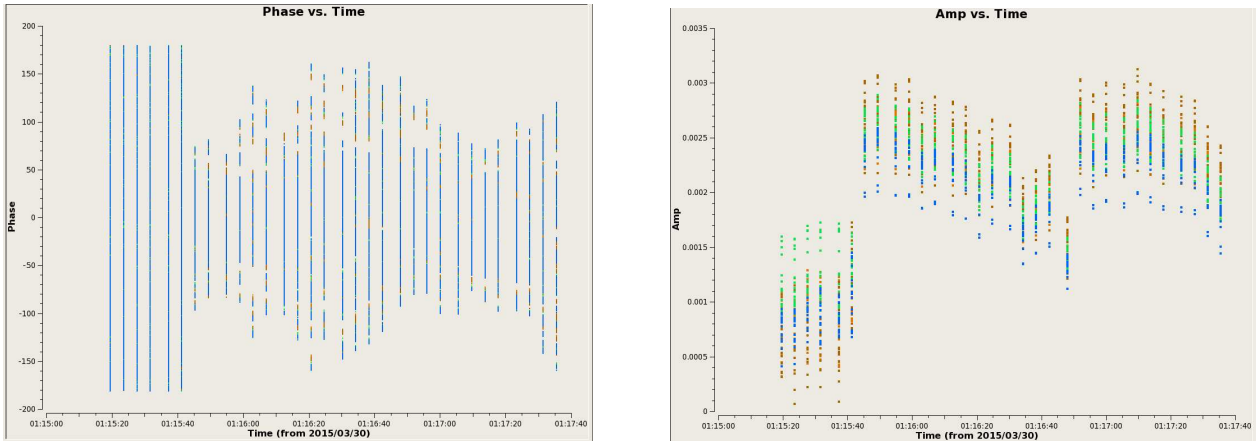

Figure 2: Same as Figure 1, but in Band 6. Data source: uid://A002/X9cdda2/X25e.

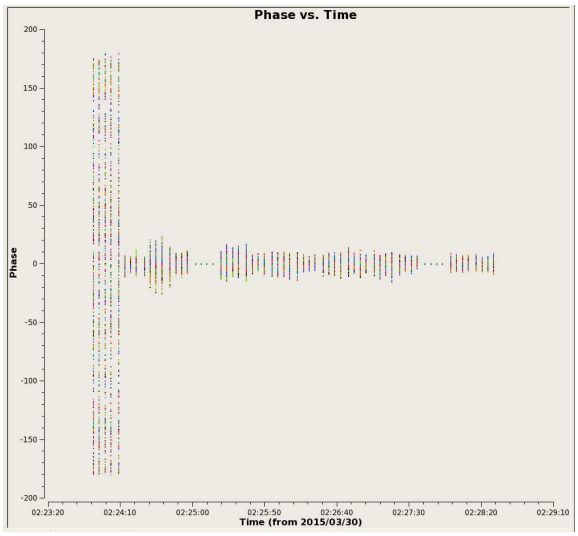

Figure 3: Phase as a function of time during Band 6 observations of the quasar 3C273 on 2015 March 30. Both the fast and slow phasing loops were active during this observation. Baselines between all phased antennas are shown. Colors indicate different baselines. Data from both the XX and YY polarizations and all four independent correlator quadrants are shown. Data on all baselines were corrupted during two scans (near 02:25:00 UT and 02:27:40 UT), resulting in spurious zero-valued phases. Data source: uid://A002/X9cdda2/X3b8.

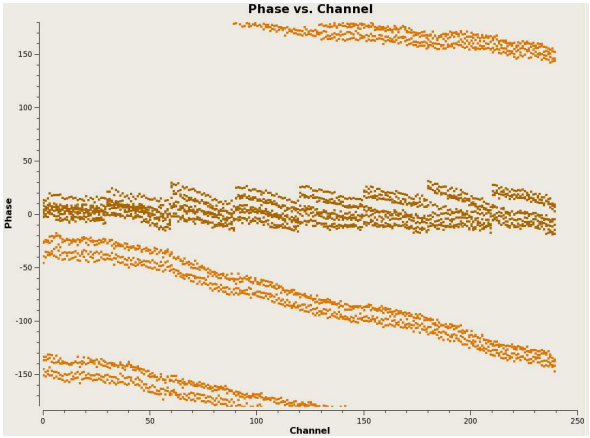

Figure 4: Example of a Band 3 cross-power spectrum on a baseline between the reference antenna and an antenna that was part of the phased sum. Data are shown for a single correlator quadrant (baseband 2), XX and YY polarization. Two scans (each comprised of four subscans) are shown. The orange symbols represent data prior to phase-up and show a phase gradient as a function of frequency as a result of the suppression of the default front-end delay corrections. The brown points show the data after phasing corrections were computed and applied in each of eight spectral regions. Because the corrections are computed from subsets of the data averaged over one-eighth of the band, small residual phase slopes remain across each of these eight regions in the spectral data. Data source: uid://A002/X9cdda2/X37.

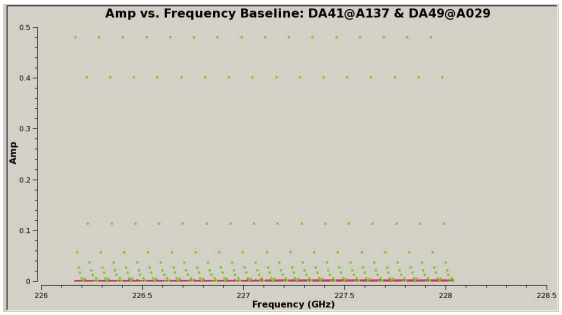

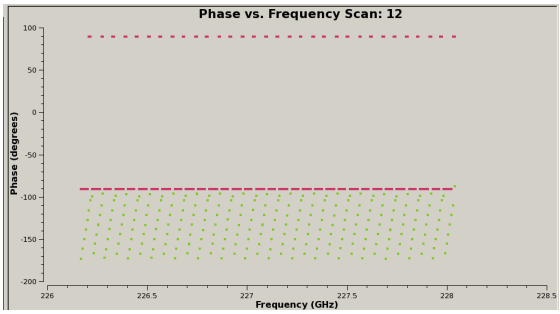

Figure 5: Example of a corrupted cross-correlation spectrum obtained on March 30 during a Band 6 VLBI fringe test. Amplitudes as a function of frequency are shown on the left and phases as a function of frequency on the right for the baseline between antennas DA41 and DA49. The two colors designate the data from the two different commanded correlator quadrants. All baselines and both polarizations were corrupted during the affected scan. Data source: uid://A002/X9cdda2/X553.

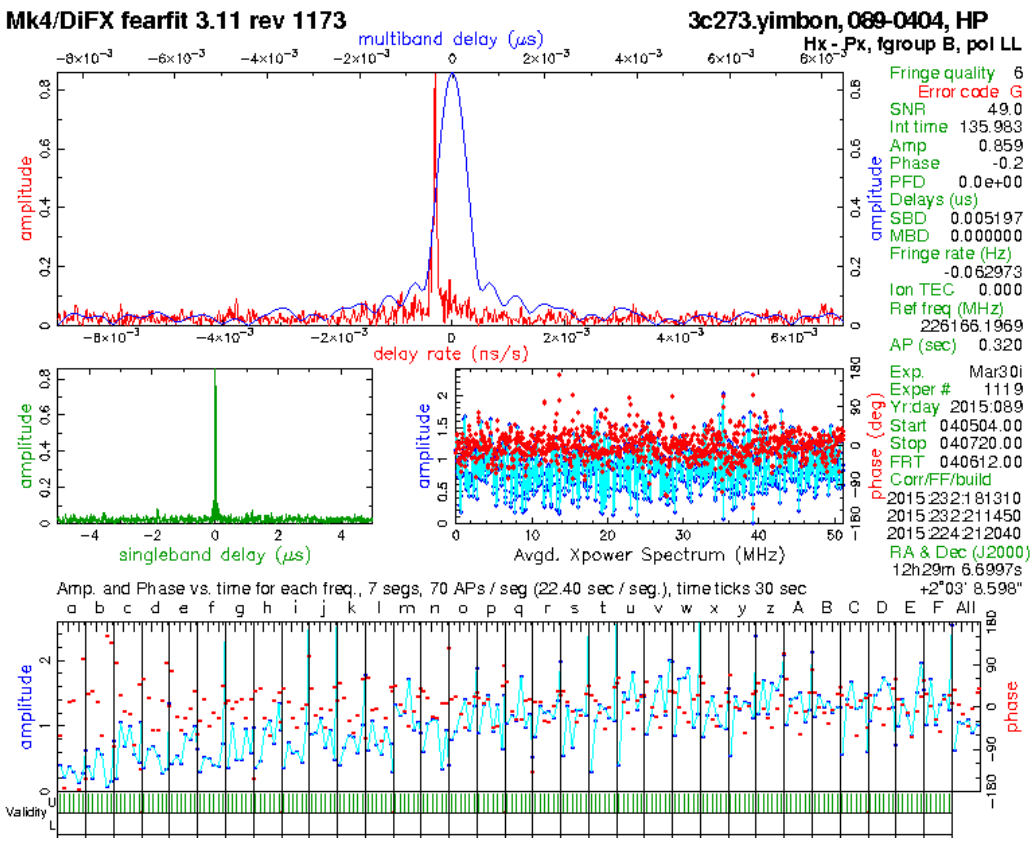

Figure 6: Band 6 VLBI fringe detection on the source 3C273, obtained on a baseline between the IRAM 30-m antenna on Pico Veleta, Spain and phased ALMA. The data were obtained on 2015 March 30. There were nine 12-m ALMA antennas in the phased array. Approximately 136 seconds of data are shown. The high signal-to-noise ratio (∼49) of the correlation between the Pico Veleta left circular polarization and the ALMA linear (XX) polarization on this very long baseline (∼9770 km) is evident from the clear peaks in the delay rate (red curve, top panel), in the single-band delay (green curve, center-left panel) and in the multi-band delay (blue curve, top panel). The center-right panel shows amplitude (blue) and phase (red), averaged over all baseband channels at a resolution of 100 kHz. (The VLBI correlation was performed at 3.125 kHz resolution). The lower plot shows amplitude (blue) and phase (red) as a function of time for each of the 32 51-MHz frequency channels. (The wings of the 62.5 MHz ALMA TFB channels were not included). Data source: uid://A002/X9cdda2/X578.

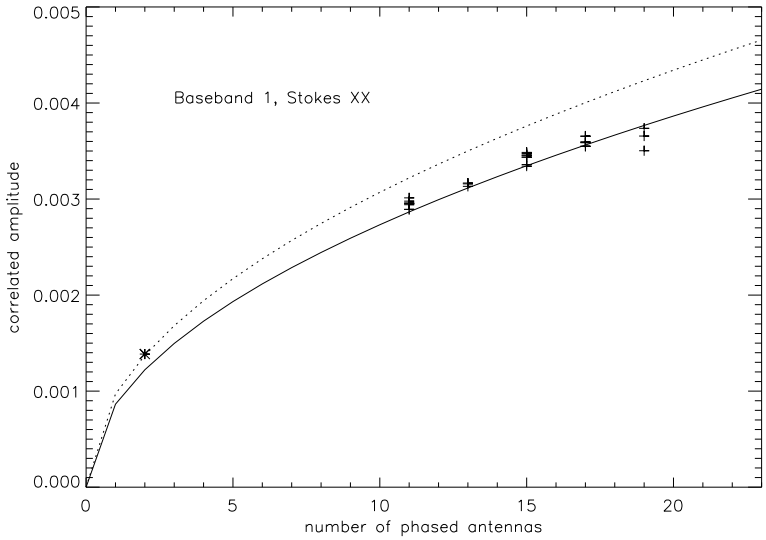

Figure 7: Sample results from a "step scan" test, carried out on 2015 March 31 on the source 0522-364 in Band 6. Data for baseband 1, polarization XX are shown. At the beginning of the ∼12-minute observation, the phased array contained 19 antennas; as the observation progressed, pairs of antennas were sequentially removed from the phased array. Crosses indicate measurements of the correlated amplitude on a baseline between the comparison antenna DA45 and the phased sum "antenna" on 16-second intervals of data. For comparison, the asterisk shows the mean correlated amplitude measured over all baselines between antennas used in the phased sum; this effectively measures the mean correlated amplitude for an array of two phased antennas. The dotted line shows the predicted amplitude increase for larger arrays on antennas. In contrast, the solid curve shows a *fit* to individual measurements between comparison antenna DA45 and the phased sum of the form $y = \epsilon_{\rm q}\sqrt{N_{\rm A}}$, where ϵ_q=0.89 is scaling factor and $N_{\rm A}$ is the number of phased antennas. In this example, all of the plotted points (asterisk and crosses) suffer inherent amplitude losses of ∼7% owing to residual RMS fluctuations in the phases of each antenna. However, the offset between the two plotted curves shows that an additional efficiency loss of ∼11% occurs during computation of the phased sum signal from the individual antenna signals. See §3.4.1 text for additional discussion. Data source: uid://A002/X9ceec1/Xb0.